

A reflow process for glass microlens array fabrication by use of precision compression molding

This content has been downloaded from IOPscience. Please scroll down to see the full text.

2008 J. Micromech. Microeng. 18 055022

(<http://iopscience.iop.org/0960-1317/18/5/055022>)

View [the table of contents for this issue](#), or go to the [journal homepage](#) for more

Download details:

IP Address: 147.188.128.74

This content was downloaded on 05/06/2015 at 09:35

Please note that [terms and conditions apply](#).

A reflow process for glass microlens array fabrication by use of precision compression molding

Yang Chen¹, Allen Y Yi¹, Donggang Yao², Fritz Klocke³ and Guido Pongs³

¹ Department of Industrial, Welding and Systems Engineering, The Ohio State University, Columbus, OH, USA

² School of Polymer, Textile & Fiber Engineering, Georgia Institute of Technology, Atlanta, GA, USA

³ Fraunhofer Institute for Production Technology, Aachen, Germany

E-mail: yi.71@osu.edu

Received 26 December 2007, in final form 2 March 2008

Published 8 April 2008

Online at stacks.iop.org/JMM/18/055022

Abstract

A novel low-cost, high-volume fabrication method for glass microlens arrays was developed by combining compression molding and thermal reflow processes. This fabrication process includes three major steps—i.e., fabrication of glassy carbon molds with arrays of micro size holes, glass compression molding to create micro cylinders on a glass substrate, and reheating to form microlens arrays. As compared to traditional polymer microlens arrays, glass microlens arrays are more reliable and therefore may be used in more critical applications. In this research, microlens arrays with different surface geometries were successfully fabricated on a P-SK57 ($T_g = 493^\circ\text{C}$) glass substrate using a combination of the compression molding and thermal reflow processes. The major parameters that influence the final lens shape, including reheating temperature and holding time, were studied to establish a suitable fabrication process. A numerical simulation method was developed to evaluate the fabrication process. Finally, both surface geometry and optical performance of the fabricated glass microlens arrays were analyzed.

(Some figures in this article are in colour only in the electronic version)

1. Introduction

In recent years, interest in microlens array fabrication has increased dramatically for their wide applications in optoelectronics and optical communication [1]. Different methods have been developed for fabricating microlens arrays, such as photoresist thermal reflow [2], polymer replication hot embossing [3] and roller embossing [4], excimer laser ablation [5], direct reactive ion etching (RIE) [6], mechanical ultraprecision machining [7] and glass compression molding [8]. Compared with microlens arrays using polymeric materials, glasses are more reliable due to their high transition temperature (T_g), chemical stability and good mechanical properties [9]. Therefore, glass microlens arrays can be used in harsh environments such as high temperature conditions. However, the aforementioned microlens array fabrication methods were mainly designed for polymeric

materials. Although excimer laser ablation and direct RIE etching may be used to fabricate glass microlens arrays, they are not mass manufacturing methods and therefore not suitable for high-volume production. Compared with these fabrication processes, glass compression molding is an emerging technique that can be adopted for high-volume fabrication of precision glass optical elements [10]. This process is also suited for fabricating glass microlens arrays.

Glass compression molding is a hot forming process in which a heated raw glass blank is pressed by optically polished molds with micro patterns to create finished glass optical components. As compared with other glass micro fabrication techniques (e.g., etching, laser ablation), glass compression molding is an environmentally benign and net shape or near net shape high-volume fabrication process. The glass compression molding process has previously been evaluated for fabricating glass diffractive optics [11].

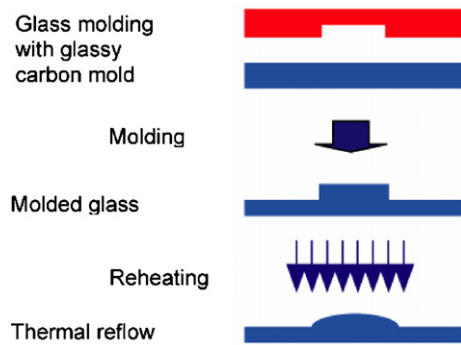


Figure 1. Illustration of the glass microlens array fabrication process, including three major steps, i.e., fabrication of molds, glass compression molding, and reheating.

Thermal reflow is a method commonly used for fabricating polymer microlens arrays for its low-cost nature, high productivity and simplicity [2]. In this process glass material is melted when processing temperature reaches a level above the transition temperature and surface tension of the molten material forces the formation of spherical geometry of the microlenses. In this paper, a hybrid fabrication method for glass microlens arrays was developed by combining the glass molding and the thermal reflow processes.

2. Fabrication process

There are three major steps involved in the fabrication of glass microlens arrays in this research: mold fabrication, glass compression molding and thermal reflow (as shown in figure 1). First of all, glassy carbon molds with arrays of micro holes were fabricated in a cleanroom lithography-etching process. Secondly, compression molding was performed to replicate the micro cylinders on a glass substrate. Finally, a reflow process was applied to thermally form the micro cylinders into microlens arrays.

In this research, glassy carbon was used as mold material for its excellent chemical stability at high temperature (up to 2000 °C) and its good optical polishability. In addition, glassy carbon can be easily fabricated using lithography and the RIE process due to its amorphous structure. These properties make glassy carbon suitable as a mold material for fabricating microlens arrays using glasses with high transition temperatures. To start, glassy carbon wafers of 2 mm thick, 50.8 mm diameter (manufactured by HTW Hochtemperatur-Werkstoffe GmbH, Gemeindewal 41, D-86672 Thierhaupten, Germany) were fabricated using lithography followed by RIE, as shown in figure 2. The photoresist was Shipley S1813 and was deposited with a thickness of 1.4 μm . The wafer was then exposed to UV radiation for 2.4 s at a density of 15 mW cm^{-2} and 365 nm wavelengths with a photolithography mask. The wafer was developed for 1 min using a MF319 developer and rinsed with de-ionized water. After development, a Ti/Ni metal layer (20/50 nm) was deposited on the glassy carbon wafer as the etching mask for the RIE process. Acetone was employed as a lift-off agent to remove

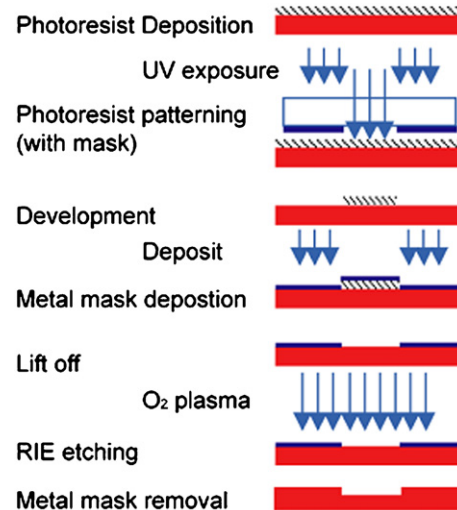


Figure 2. Micromachining process for a glassy carbon wafer.

the photoresist layer and the metal deposition that were not needed for the next etching step. A bench top RIE (Technics Micro-RIE Series 800 II) unit was used for reactive ion etching of the wafer with oxygen plasma. The pressure during etching was 150 mTorr. with an RF power of 200 W. The oxygen flow rate during etching was 20 $\text{cm}^3 \text{min}^{-1}$ and the total etching time was 30 min. The remaining metal mask was removed by acid solution after etching.

The glassy carbon molds were measured for geometric and surface finish. Figure 3 shows SEM images of the glassy carbon molds, and figure 4 is a cross-sectional view of the glassy carbon mold measured by a Taylor Hobson PGI 1250 profilometer along the diameter direction. To fabricate the microlens arrays used in this research, glassy carbon molds with 100 μm diameter microholes were etched to 10 μm deep, as shown in figure 4. The pitch distance was 200 μm in this mold design.

After the glassy carbon molds were completed, glass compression molding experiments for micro glass optical components were performed on a Toshiba GMP 211 V machine at the Fraunhofer Institute for Production Technology (IPT), Aachen, Germany. The schematic in figure 5 illustrates four major steps of the process. The glass blanks used in this experiment were optically polished on both sides. The shaded component in the figure is a P-SK57 glass blank.

The compression molding process began with heating of the entire mold assembly and the glass blank to the preset forming temperature (565 °C in this research). The lower mold was then pushed upward at a velocity of 0.5 mm min^{-1} to the forming position. After reaching the molding temperature, the entire system was kept for 300 s (soaking time) to ensure uniform temperature distribution inside the machine. The molding force was kept constant at 2 kN for 40 s to ensure that complete contact was made between the glassy carbon mold and the glass workpiece. A 200 N constant load was applied from the start of the cooling stage. The applied load was removed after cooling for 40 s. Once the mold and

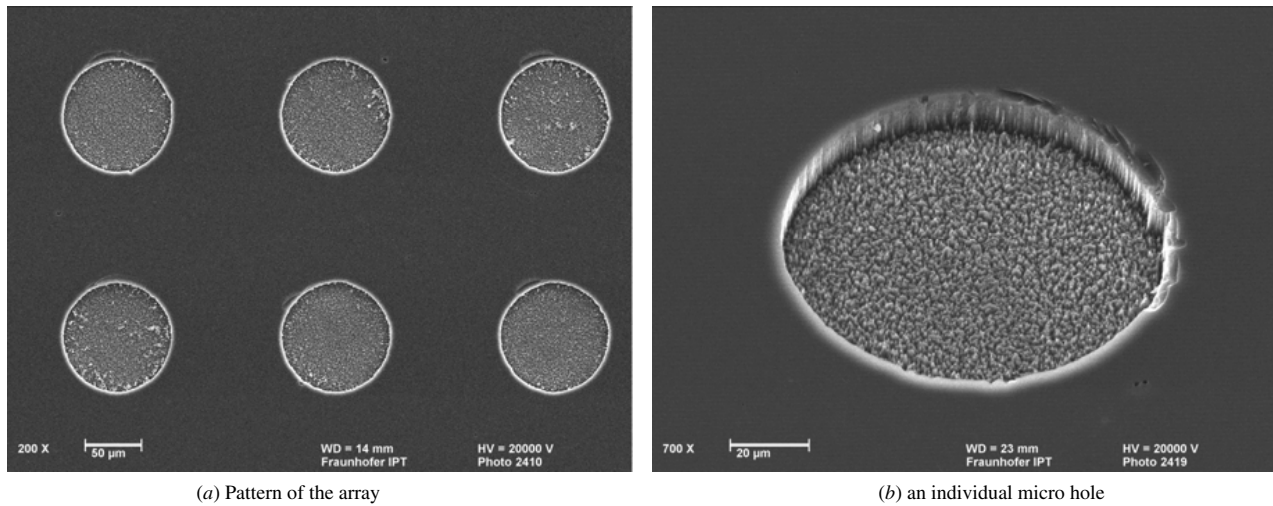


Figure 3. Fabricated glassy carbon molds measured by SEM show (a) an array of 100 μm diameter microholes with 200 μm pitch, and (b) an individual microhole on the glassy carbon mold.

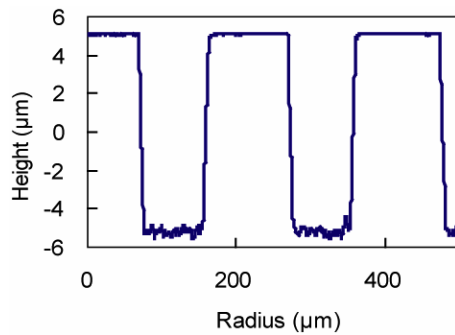


Figure 4. The dimensions of glassy carbon molds measured by a Taylor Hobson profilometer. The result shows that the diameter is 100 μm , and the depth is 10 μm .

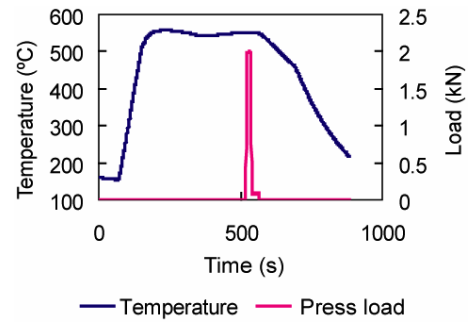


Figure 6. Molding temperature and press load time history for a glass microlens array, with 565 $^{\circ}\text{C}$ molding temperature, 300 s soaking time and 2 kN molding force.

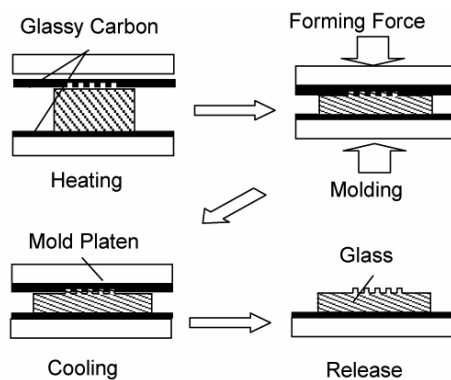


Figure 5. Schematic illustration of glass compression molding, including heating, molding, cooling and release.

glass temperature was lowered to approximately 200 $^{\circ}\text{C}$, the glass workpiece was released and cooled to room temperature naturally. The process parameters were shown in figure 6. During this experiment, a vacuum was applied at the beginning to ensure that no air remained in the gap between the mold and

glass workpiece. This was immediately followed by nitrogen purge to further remove oxygen residual. During the cooling stage, the nitrogen flow rate was adjusted to control the cooling speed.

After the molding process was completed, the glass workpiece with micro cylinders was re-heated to a temperature that was higher than its glass transition temperature and was kept at this temperature for a pre-determined amount of time (400 s in the experiment performed at 600 $^{\circ}\text{C}$) to achieve the desired surface curve shape. Controlled cooling was performed (the same as in molding process). At the soaking temperature, glass behaves as a viscoelastic material [14], which is strongly time and temperature dependent. Microlenses with precise surface geometry may be created at different soaking temperatures (which affect surface tension) and soaking times. In this research, varied reheating temperatures from 560 $^{\circ}\text{C}$ to 620 $^{\circ}\text{C}$ and soaking times from 100 to 400 s were used to evaluate the effect of process parameters. Figure 7 shows a thermal history for the reheat thermal reflow process under 600 $^{\circ}\text{C}$ reheating temperature with 4 s soaking time.

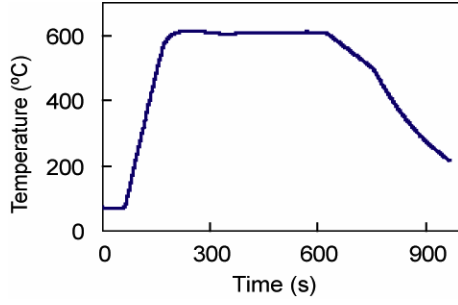


Figure 7. Thermal time history for the reheating process with 600 °C reflow temperature and 400 s holding time.

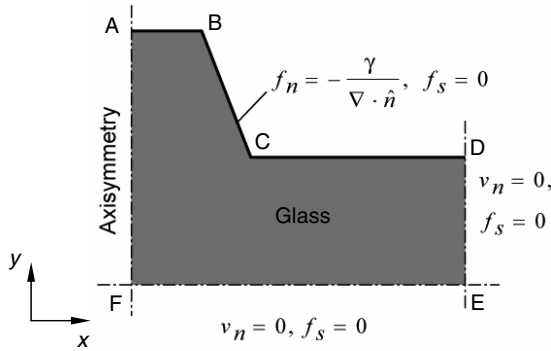


Figure 8. Surface tension driven reflow model. In the model, the dimensions along the x - and y -axes have different scales; along the x -axis, $FE = 150 \mu\text{m}$, and along the y -axis, $AF = 20 \mu\text{m}$.

3. Numerical simulation of the reflow process

Reflow of a molten glass article can be driven by gravity and/or surface tension. The relative importance of each factor depends on the size of the flow domain. To compare the two effects, one may conduct an order of magnitude analysis of a fluid domain with a characteristic dimension of D . The work

done by surface tension can be estimated to be

$$\Delta S = D^2 \gamma, \quad (1)$$

where γ is the surface tension, and the work done by gravity can be estimated to be

$$\Delta G = D^4 \rho g, \quad (2)$$

where ρ is the density and g is the gravitational acceleration. Therefore the relative importance of these effects can be compared using a dimensionless group defined as

$$Sg = \frac{\Delta S}{\Delta G} = \frac{\gamma}{D^2 \rho g}. \quad (3)$$

In microlens molding, the characteristic dimension is of the order of $10 \mu\text{m}$, resulting in an Sg of the order of 10^5 . Therefore only surface tension needs to be considered in the reflow process for a microlens.

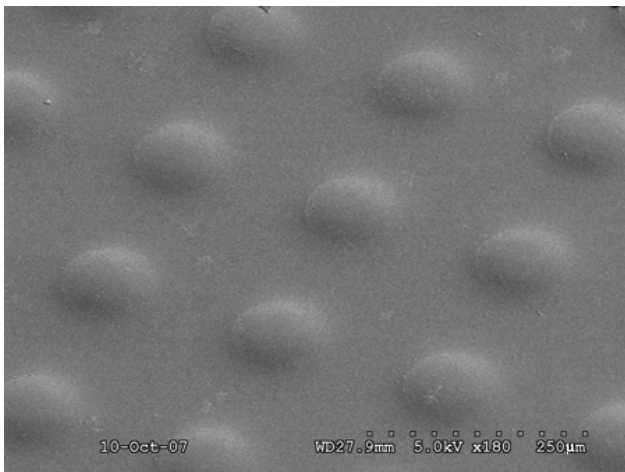
Isothermal surface tension driven flow can be approximated using a creep flow model. In this case, the material is considered to be a purely viscous material, and compressibility is neglected. The simplified conservation equations are

$$\nabla \cdot \underline{v} = 0, \quad (4a)$$

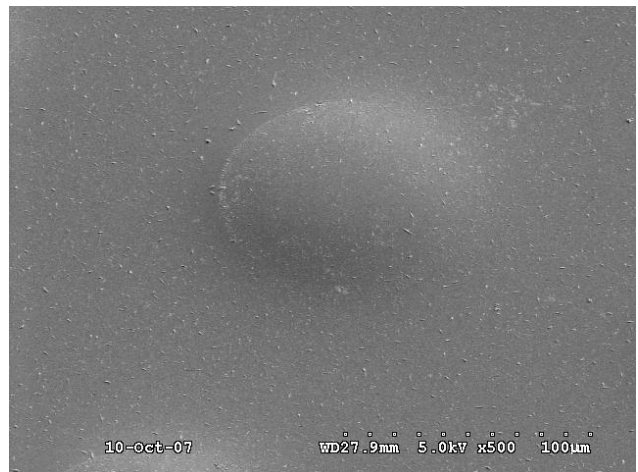
$$-\nabla p + \nabla \cdot [\eta(\nabla \underline{v} + \nabla \underline{v}^T)] = 0, \quad (4b)$$

where p is the pressure, η is the viscosity and \underline{v} is a velocity vector.

The geometry and the boundary conditions used in the reflow model are shown in figure 8. It was assumed that the surface tension induced deformation is local to the microlens. The fluid domain (i.e., glass) is axisymmetric. Due to this axisymmetry, only half a cross-section is shown in the model. The boundary conditions on the symmetries are zero normal velocity and zero tangential stress, i.e., $v_n = \hat{n} \cdot \underline{v} = 0$ and $f_s = \hat{n} \cdot \underline{\underline{\sigma}} \cdot \hat{s} = 0$, where \hat{n} and \hat{s} are unit normal and tangential vectors and $\underline{\underline{\sigma}}$ is the total stress tensor. On the free surface, surface tension causes a net normal stress



(a)



(b)

Figure 9. SEM images for the fabricated microlens array on a glass substrate, after thermal reflow at 610 °C with 400 s soaking time: (a) molded lens array; (b) an individual lens.

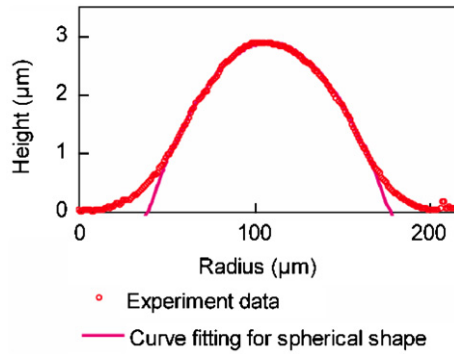


Figure 10. Surface geometry of a microlens after thermal reflow (610 °C and 400 s). The circular dotted line is the measured data from the Veeco scan, and the solid line is the curve fitting for spherical shape of 830 μm radius.

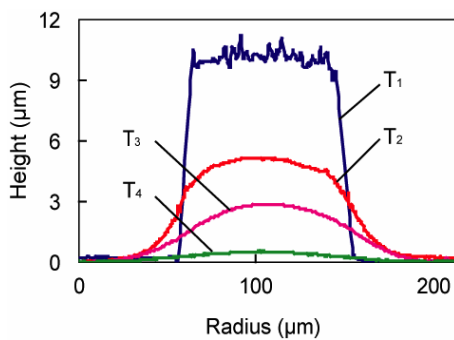


Figure 11. Surface geometry at different thermal reflow temperature. Four different results at different reflow temperatures are shown: $T_1 = 560$ °C, $T_2 = 600$ °C, $T_3 = 610$ °C and $T_4 = 620$ °C.

on the surface, indicated as $f_n = -\frac{\gamma}{\nabla \cdot \hat{n}}$, where $\nabla \cdot \hat{n}$ is the curvature. The governing equations and boundary conditions were implemented using Polyflow, a commercially available finite element analysis software package for polymer/glass molding and forming. The mesh size and time step used were 1 μm and 0.01 s. Further refinement of these parameters did not change the accuracy of the solution.

4. Results and discussion

4.1. Geometry measurement

The glass microlens arrays fabricated using thermal reflow were measured by SEM and a Veeco NT3300 optical profiler to evaluate the fabrication results. To observe the surface morphology using SEM, a thin layer of gold was sputter coated on the glass substrate for 2 min under 20 mA current using an Emitech K550X coater (Empdirect Products Inc., 704/17033 Butte Creek, Houston, TX 77090). Figure 9 shows SEM images of the microlens array after the thermal reflow step.

Figure 10 shows the Veeco scan of the surface geometry for a microlens along the diameter direction after thermal reflow at 610 °C with 400 s soaking time. The dotted line is the curve measured in the experiment and the solid line is from curve fitting for a spherical shape of 830 μm radius. The

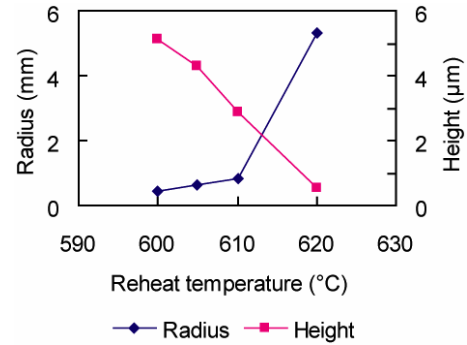


Figure 12. Radius and height of microlenses at different thermal reflow temperature. With the increasing of reheating temperature, the radius of the microlens increases and the height of the microlens decreases.

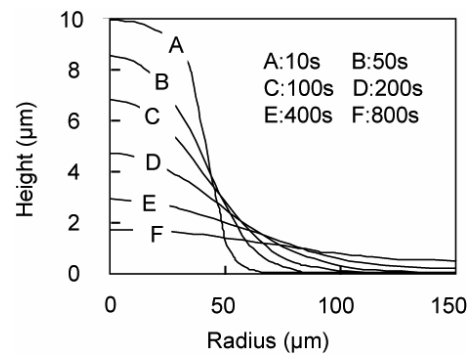


Figure 13. Simulation results showing the evolution of the microlens geometry during surface tension driven reflow.

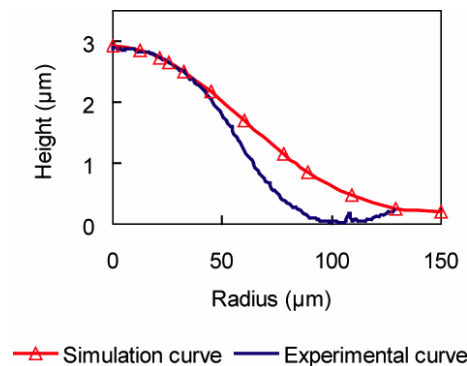


Figure 14. Comparison between simulation and experimental results.

microlens itself is about 150 μm in diameters and its height is 2.89 μm.

Since the viscosity of glass material is strongly temperature dependent, different thermal reflow temperatures were tested to study the influence of temperature on surface curve change. Figure 11 shows a surface curve comparison of microlens arrays fabricated at different reflow temperatures with the same soaking time. At a higher reheating temperature, glass material had a lower viscosity. Therefore a lower height of microlens array (sagittal value) was expected as in figure 12. When the reflow temperature was 560 °C or lower, there was almost no change in the surface shape from the molded

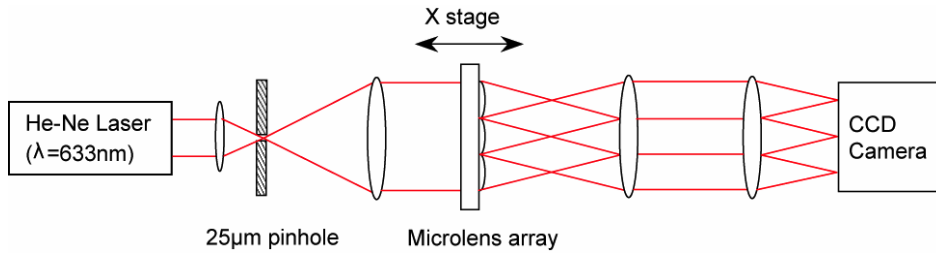
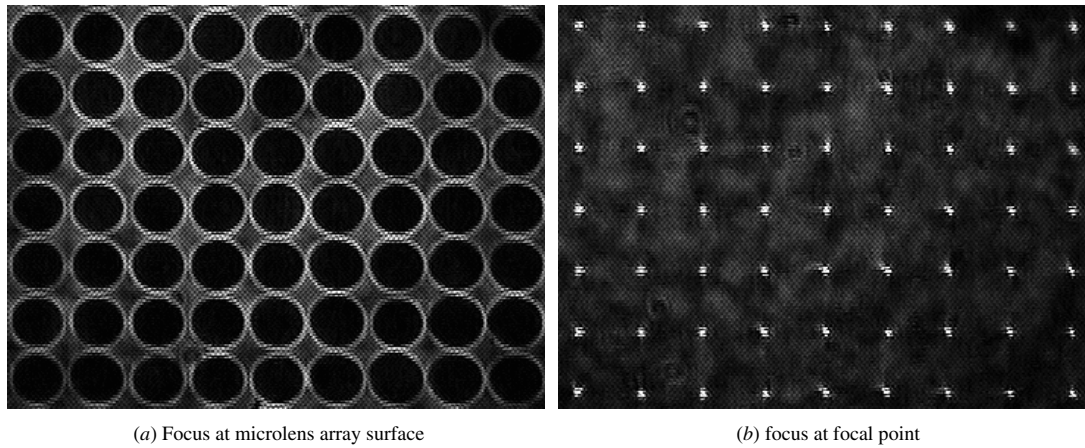


Figure 15. Optical test setup for measuring the focal length of a fabricated microlens array.



(a) Focus at microlens array surface

(b) focus at focal point

Figure 16. Images of the light spot array produced by the microlens; (a) is the image of a CCD camera focused at the microlens array surface, and (b) is the image focused at the microlens array's focal point. The distance between these two focal surfaces gives the focal length of the microlens array.

glass microcylinders. On the other hand, when the reflow temperature was more than 620 °C, the shape of the microlenses became effectively flat. Therefore, for P-SK57 glass, the reheating temperature for the thermal reflow process should be controlled between 600 °C and 610 °C (a relatively easy task on the GMP-211 V glass molding machine), as shown in figure 11.

4.2. Reflow simulation results

The dimensions of the compression molded microcylinders, about 10 μm in height and 100 μm in diameter with a slope on the side, were taken as the dimensions for the initial geometry in the model. The typical surface tension of molten glass is approximately 0.3 N m⁻¹ [15]. The viscosity of molten P-SK57 glass was previously characterized [12], governed by the following equation

$$\log \eta(T) = A + \frac{B}{T - T_0}, \quad (5)$$

where A , B and T_0 are model coefficients and for this material are -3.556, 2917.3 and 306.4, respectively. The calculated viscosity at 610 °C is 10⁶ Pa s. However, the simulation results with these parameters did not agree with the experimental observations. Instead, good agreement was obtained at a slightly lower viscosity of 3 × 10⁵ Pa s. The simulated reflow for $\eta = 3 \times 10^5$ Pa s and $\gamma = 0.3$ N m⁻¹ at a different time is shown in figure 13. At these parameters, reflow would

occur at a similar time scale as observed in the experiments, as shown in figure 14 for a reflow process at 610 °C and 400 s holding time. This discrepancy may be explained considering the deviation of the actual temperature inside the mold, that is, the temperature measured outside the mold cavity could be significantly lower than the actual molding temperature. From equation (5), the temperature corresponding to $\eta = 3 \times 10^5$ Pa s is approximately 630 °C. The underestimated glass molding temperature predicted a higher viscosity and consequently a slower reflow process. Furthermore, the surface tension used in the simulation was an estimate from the literature and therefore could bring in additional calculation errors.

4.3. Focal length measurement

To investigate the performance of the fabricated microlens arrays, the focal lengths of the microlenses were measured by using the system shown in figure 15. In the test setup, a He-Ne laser (wavelength 632.8 nm) was employed as the light source and a charge coupled device (CCD) was used as an image collector. The fabricated microlens array was placed on a precision stage, which can be moved along the optical axis direction. First, the microlens array was manually moved to a position where the focus was on the flat surface of the microlens array workpiece (figure 16(a)). Then the stage was adjusted to move the microlens array away from the CCD camera until sharp focused spots were detected by the CCD camera (figure 16(b)). Figure 16 shows the image and focused

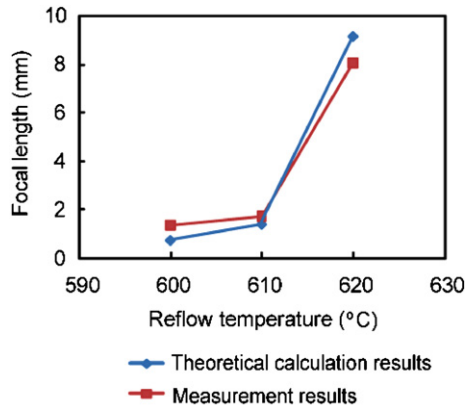


Figure 17. Focal length comparison between optical measurement and theoretical calculation under different thermal reflow temperatures.

light spots detected by the CCD camera for one of the glass microlens arrays, which was fabricated using thermal reflow at 610 °C with 400 s holding time. The distance between these two positions gives the focal length of the microlens array.

The focal length of the microlens array can be analytically determined approximately by using the radius of curvature (R) and the refractive index of P-SK57 glass with the equation below:

$$f = \frac{R}{n - 1}. \quad (6)$$

The refractive index of P-SK57 for 632.8 nm wavelengths is 1.5849 according to the data sheet from Schott glass [12]. The calculated radius of curvature after thermal reflow (610 °C and 400 s) is 830 μm according to the curve fitting results, as shown in figure 10. Therefore, the focal length of this microlens was 1.42 mm by using equation (6). The measurement result of focal length using the above method is 1.75 mm. Figure 17 shows a comparison between the measurement results and theoretical calculation with equation (6) under a different thermal reflow temperature. The difference between measurement and theoretical calculation may come from measurement errors in focal length and geometrical curvature measurement.

5. Conclusions

A new method for high-volume microlens array production using P-SK57 glass was presented by combining the glass compression molding and thermal reflow processes. The quality of the glass lens surface geometry was measured using a stylus profilometer and it was discovered that glass microlens arrays with 150 μm in diameter and 2.89 μm sagittal height were fabricated using thermal reflow at 610 °C with 400 s soaking time. Furthermore, by controlling reheating temperature and soaking time, microlens arrays with different radii and focal lengths were created. Specifically, four different reheating temperatures from 600 °C to 620 °C were tested to study the relationship between reheating temperature and microlens curve shape. According to the experimental

results, a desirable microlens curve could be obtained within the temperature range with a 400 s holding time. At a higher reheating temperature, a lens array with a lower sagittal height was expected. Numerical simulation was performed to evaluate and characterize the fabrication process. The simulation results were compared with experimental data. It was found that minor discrepancies exist between experiments and simulation results. These differences were explained by temperature measurement error and surface tension deviation. Finally, the focal lengths of fabricated glass microlens arrays were measured using an optical setup. Glass microlens arrays with focal lengths from 1.38 to 8.04 mm were obtained using different thermal reflow temperatures. The experimental results matched well with the analytical calculation. These results indicate that the method presented in this study may be used for fabricating glass microlens arrays with controllable diameters and sagittal height with good optical performance. Furthermore, as a high-throughput replication process, the new process is suitable for mass production of various micro glass optical elements at a low cost.

Acknowledgments

This material is partially based on work supported by the National Science Foundation under grant no CMMI 0547311. Any opinions, findings and conclusions or recommendations expressed in this material are those of the authors and do not necessarily reflect the views of the National Science Foundation. The glass molding experiments were conducted at the Fraunhofer Institute for Production Technology in Aachen, Germany. FK and GP would like to acknowledge the support of the Transregionaler Sonderforschungsbereich 4 (SFB/TR4) project from Deutsche Forschungsgemeinschaft (DFG). YC and AYY also acknowledge the financial support for travel to Aachen, Germany from NSF's International Research and Education in Engineering (IREE) program under the same grant no (CMMI 0547311).

References

- [1] Hutley M C, Stevens R F and Daly D 1991 Microlens arrays *Phys. World* **4** 27–32
- [2] Daly D, Stevens R F, Hutley M C and Davies N 1990 The manufacture of microlenses by melting photoresist *Meas. Sci. Technol.* **1** 759–66
- [3] Shen Y K 2006 A novel fabrication method for the mold insert of microlens arrays by hot embossing molding *Polym. Eng. Sci.* **10.1002** 1797–803
- [4] Chang C Y, Yang S Y and Sheh J L 2006 A roller embossing process for rapid fabrication of microlens arrays on glass substrates *Microsyst. Technol.* **12** 754–9
- [5] Wakaki M, Komachi Y and Kanai G 1998 Microlens and microlens arrays formed on a glass plate by use of a CO₂ laser *Appl. Opt.* **37** 627–31
- [6] Savander P 1994 Microlens arrays etched into glass and silicon *Opt. Lasers Eng.* **20** 97–107
- [7] Yi A Y and Li L 2005 Design and fabrication of a microlens array by use of a slow tool servo *Opt. Lett.* **30** 1707–9
- [8] Firestone G C and Yi A Y 2005 Precision compression molding of glass microlenses and microlens arrays—an experimental study *Appl. Opt.* **44** 6115–22

- [9] Ottevaere H, Cox R, Herzig H P, Miyashita T, Naessens K, Taghizadeh M, Vlkel R, Woo H J and Thienpont H 2006 Comparing glass and plastic refractive microlenses fabricated with different technologies *J. Opt. A: Pure Appl. Opt.* **8** S407–29
- [10] Maschmeyer R O, Andrysick C A, Geyer T W, Meissner H E, Parker C J and Sanford L M 1983 Precision molded glass optics *Appl. Opt.* **22** 2413–5
- [11] Yi A Y, Chen Y, Klocke F, Pongs G, Demmer A, Grewell D and Benatar A 2006 A high volume precision compression molding process of glass diffractive optics by use of a micromachined fused silica wafer mold and low T_g optical glass *J. Micromech. Microeng.* **16** 2000–5
- [12] http://www.us.schott.com/optics_devices/english/products/materials_for_molding.html.
- [13] Yi A Y and Raasch T W 2005 Design and fabrication of a freeform phase plate for high order ocular aberration correction *Appl. Opt.* **44** 6869–76
- [14] Jain A, Firestone G C and Yi A Y 2005 Viscosity measurement by cylindrical compression for numerical modeling of precision lens molding process *J. Am. Ceram. Soc.* **88** 2409–14
- [15] Zhilin A A, Kanchiev Z I, Tatarintsev B V and Yagmurov V K 2003 Measuring the surface tension of glass in the temperature region of softening and viscous flow *J. Opt. Technol.* **70** 888–91